

A novel clustering algorithm based on quantum games

This article has been downloaded from IOPscience. Please scroll down to see the full text article.

2009 J. Phys. A: Math. Theor. 42 445303

(<http://iopscience.iop.org/1751-8121/42/44/445303>)

View [the table of contents for this issue](#), or go to the [journal homepage](#) for more

Download details:

IP Address: 171.66.16.156

The article was downloaded on 03/06/2010 at 08:19

Please note that [terms and conditions apply](#).

A novel clustering algorithm based on quantum games

Qiang Li, Yan He and Jing-ping Jiang

College of Electrical Engineering, Zhejiang University, Hang Zhou, Zhejiang 310027,
People's Republic of China

E-mail: anjuh@cqu.edu.cn, heyang@zju.edu.cn and eejiang@zju.edu.cn

Received 29 March 2009, in final form 9 August 2009

Published 8 October 2009

Online at stacks.iop.org/JPhysA/42/445303

Abstract

Enormous successes have been made by quantum algorithms during the last decade. In this paper, we combine the quantum game with the problem of data clustering, and then develop a quantum-game-based clustering algorithm, in which data points in a dataset are considered as players who can make decisions and implement quantum strategies in quantum games. After each round of a quantum game, each player's expected payoff is calculated. Later, he uses a link-removing-and-rewiring (LRR) function to change his neighbors and adjust the strength of links connecting to them in order to maximize his payoff. Further, algorithms are discussed and analyzed in two cases of strategies, two payoff matrixes and two LRR functions. Consequently, the simulation results have demonstrated that data points in datasets are clustered reasonably and efficiently, and the clustering algorithms have fast rates of convergence. Moreover, the comparison with other algorithms also provides an indication of the effectiveness of the proposed approach.

PACS numbers: 89.75.-k, 03.67.-a, 02.50.Le, 43.60.Lq

1. Introduction

Quantum computation is an extremely exciting and rapidly growing field. More recently, an increasing number of researchers with different backgrounds, ranging from physics, computer sciences and information theory to mathematics and philosophy, have been involved in researching properties of quantum-based computation [1]. During the last decade, a series of significant breakthroughs have been made. One was that in 1994 Peter Shor surprised the world by proposing a polynomial-time quantum algorithm for integer factorization [2], while in the classical world the best-known classical factoring algorithm works in superpolynomial time. Three years later, in 1997, Lov Grover proved that a quantum computer could search an unsorted database in the square root of the time [3]. Meanwhile, Brassard *et al*

combined ideas from Grover's and Shor's quantum algorithms to propose a quantum counting algorithm [4].

In recent years, much interest has focused on quantum game theory and considerable work has been done. For instance, Meyer [5] studied the Penny Flip game in the quantum world firstly. His result showed that if a player was allowed to implement quantum strategies, he would always defeat his opponent who played the classical strategies and increase his expected payoff as well. Eisert *et al* [6] quantized the prisoners' dilemma and demonstrated that the dilemma could be escaped when both players resort to quantum strategies. Flitney *et al* [7] generalized Eisert's result, the miracle move, i.e. the result of the game would move toward the quantum player's preferred result, while the other player used classical strategies. Marinatto *et al* [8] investigated the Battle of the Sexes game in quantum domain. Their result showed that there existed a unique equilibrium in the game, when the entangled strategies were allowed. Lee *et al* [9] reported that the quantum game is more efficient than the classical game, and they found an upper bound for this efficiency. Besides, some experiments about the quantum games have also been implemented on different quantum computers [10–12]. For more details about quantum games, see [13].

Successes achieved by quantum algorithms make us guess that powerful quantum computers can figure out solutions faster and better than the best-known classical counterparts for certain types of problems. Furthermore, it is more important that they offer a new way to find potentially dramatic algorithmic speed-ups. Therefore, we may ask naturally: can we construct quantum versions of classical algorithms or present new quantum algorithms to solve the problems in pattern recognition faster and better on a quantum computer? Following this idea, some researchers have proposed their novel methods and demonstrated exciting results [14–18].

In addition, data clustering is a main branch of pattern recognition, which is widely used in many fields such as pattern analysis, data mining, information retrieval and image segmentation. In these fields, however, there is usually little *a priori* knowledge available about the data. In response to these restrictions, clustering methodology come into being which is particularly suitable for the exploration of interrelationships among data points. Data clustering is the formal study of algorithms and methods for grouping or classifying unlabeled data points [19]. In other words, its task is to find the inherent structure of a given collection of unlabeled data points and group them into meaningful clusters [19]. In this paper, we attempt to combine the quantum game with the problem of data clustering in order to establish a novel clustering algorithm based on quantum games. In our algorithms, unlabeled data points in a dataset are regarded as players who can make decisions in quantum games. On a time-varying network formed by players, each player is permitted to use quantum strategies and plays a 2×2 entangled quantum game against each one of his neighbors, respectively. Later, he applies a link-removing-and-rewiring (LRR) function to remove the links of neighbors with small payoffs and create new links to neighbors with higher payoffs at the same time. Furthermore, the strength of links between a player and his neighbors is different from one another, which is updated by the Grover iteration. During quantum games, the structure of network and the strength of links between players tend toward stability gradually. Finally, if each player only connects to the neighbor with the highest strength, the network will naturally divide into several separate parts, each of which corresponds to a cluster.

The remainder of this paper is organized as follows: section 2 introduces some important concepts about the quantum computation and the quantum prisoners' dilemma briefly. In section 3, the algorithms are established in two cases of strategies, payoff matrices and link-removing-and-rewiring (LRR) functions, and then they are elaborated and analyzed. In section 4, the relationship between the number of nearest neighbors and the number of clusters

Table 1. Payoff matrix for the prisoners' dilemma.

	$C = 0$	$D = 1$	
$C = 0$	$R = 3$	$S = 0$	
$D = 1$	$T = 5$	$P = 1$	

is discussed. Next, the effect of the cost in the SD-like payoff matrix is analyzed, and the relationship between the total payoffs and the rates of convergence of algorithms is explained. In section 5, those datasets used in the simulations are introduced briefly, and then results of algorithms are demonstrated. The conclusion is given in section 6.

2. Quantum computation and quantum game

2.1. Quantum computation

The elementary unit of quantum computation is called the qubit, which is typically a microscopic system, such as an atom, a nuclear spin or a polarized photon. In quantum computation, the Boolean states 0 and 1 are represented by a prescribed pair of normalized and mutually orthogonal quantum states labeled as $\{|0\rangle, |1\rangle\}$ to form a 'computational basis' [20]. Any pure state of the qubit can be written as a superposition state $\alpha|0\rangle + \beta|1\rangle$ for some α and β satisfying $|\alpha|^2 + |\beta|^2 = 1$ [20]. A collection of n qubits is called a quantum register of size n , which spans a Hilbert space of 2^n dimensions, so that 2^n mutually orthogonal quantum states can be available.

Quantum state preparations, and any other manipulations on qubits, have to be performed by unitary operations. A quantum logic gate is a device which performs a fixed unitary operation on selected qubits in a fixed period of time, and a quantum circuit is a device consisting of quantum logic gates whose computational steps are synchronized in time [20]. The most common quantum gate is the Hadamard gate, which acts on a qubit in state $|0\rangle$ or $|1\rangle$ to produce

$$\begin{cases} |0\rangle \xrightarrow{H} \frac{1}{\sqrt{2}}|0\rangle + \frac{1}{\sqrt{2}}|1\rangle \\ |1\rangle \xrightarrow{H} \frac{1}{\sqrt{2}}|0\rangle - \frac{1}{\sqrt{2}}|1\rangle, \end{cases} \quad H = \frac{1}{\sqrt{2}} \begin{pmatrix} 1 & 1 \\ 1 & -1 \end{pmatrix}. \quad (1)$$

For more details see [20, 21].

2.2. Quantum prisoners' dilemma

The prisoners' dilemma (PD), a well-known example in the classical game theory, is an abstract of many phenomena in the real world and it has been widely used in plenty of scientific fields. In this game, each of two players has two optional strategies, cooperation (C) and defection (D). Later, he chooses one strategy against the other's for maximizing his own payoff, so does the other side at the same time, but both sides do not know the opponent's strategy. As a result, each player receives a payoff which depends on his selected strategy, where the payoff matrix under different strategy profiles is described in table 1. According to the classical game theory, the strategy profile (defection, defection) is the unique Nash equilibrium [22, 23], but unfortunately it is not Pareto optimal [24].

In the quantum game, however, thanks to the quantum strategies, the dilemma in the classical game can be escaped in a restricted strategic space [6]. The physical model of quantum prisoners' dilemma presented by Eisert [6] is shown in figure 1.

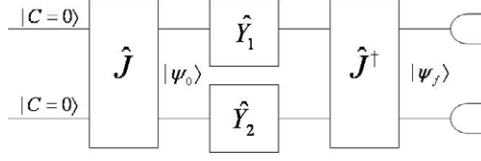


Figure 1. Block diagram of the system.

If the possible outcomes of the classical strategies, $C = 0$ and $D = 1$, are assigned to two basis vectors $\{|C = 0\rangle, |D = 1\rangle\}$ in Hilbert space, respectively, then at any time the state of the game may be represented by a vector in the space spanned by the basis $\{|00\rangle, |01\rangle, |10\rangle, |11\rangle\}$ [6]. Assume the initial state of the game is $|\psi_0\rangle = \hat{J}|00\rangle$, where \hat{J} is an entangling operator which is known to both players. For a two-player game with two pure strategies, the general form of \hat{J} may be written as [25, 26]

$$\hat{J}(\gamma) = \exp\left(i\frac{\gamma}{2}\sigma_x^{\otimes 2}\right) = I^{\otimes 2} \cos \frac{\gamma}{2} + i\sigma_x^{\otimes 2} \sin \frac{\gamma}{2} \quad (2)$$

where $\gamma \in [0, \pi/2]$ is a measure of entanglement of a game. When $\gamma = \pi/2$, there is a maximally entangled game, in which the entangling operator takes the form

$$\hat{J}(\gamma) = \frac{1}{\sqrt{2}}(I^{\otimes 2} + i\sigma_x^{\otimes 2}). \quad (3)$$

Next, each player chooses a unitary operator $\hat{Y}_1(\hat{Y}_2)$ from the strategy space $S_1(S_2)$ and operates it on the qubit that belongs to him, which makes the game in a state $(\hat{Y}_1 \otimes \hat{Y}_2)\hat{J}|00\rangle$. Specifically, the unitary operators \hat{C} and \hat{D} that correspond to the strategies, cooperation and defection, are given below [6]:

$$\hat{C} = \begin{pmatrix} 1 & 0 \\ 0 & 1 \end{pmatrix}, \quad \hat{D} = \begin{pmatrix} 0 & 1 \\ -1 & 0 \end{pmatrix}. \quad (4)$$

In the end, before a projective measurement in the basis $\{|0\rangle, |1\rangle\}$ is carried out, the final state is

$$|\psi_f\rangle = \hat{J}^\dagger(\hat{Y}_1 \otimes \hat{Y}_2)\hat{J}|00\rangle. \quad (5)$$

Thus, the player's expected payoff is written as

$$z = R|\langle\psi_f|00\rangle|^2 + S|\langle\psi_f|01\rangle|^2 + T|\langle\psi_f|10\rangle|^2 + P|\langle\psi_f|11\rangle|^2. \quad (6)$$

For more details see [6, 27].

3. Algorithm

In the section, we will combine the model of the quantum game with the problem of data clustering, and then establish clustering algorithms based on quantum games. Assume an unlabeled dataset $X = \{X_1, X_2, \dots, X_N\}$, which are distributed in an m -dimensional metric space. Each data point in the dataset is considered as a player in quantum games who can make decisions and always hope to maximize his payoff. In the metric space, there is a distance function $d : X \times X \rightarrow \mathbb{R}$, satisfying that the closer the two players, the smaller the output is. Based on the distance function, a k -nearest-neighbor (knn) network as a weighted and directed network, $G_0(X, E_0, d)$, may be created among data points by adding k edges directed toward its k nearest neighbors for each player.

Definition 1. If there is a set X with N players, $X = \{X_1, X_2, \dots, X_N\}$, the weighted and directed knn network, $G_0(X, E_0, d)$, is created as below:

$$\begin{cases} X = \{X_i, i = 1, 2, \dots, N\} \\ E_0 = \bigcup_{i=1}^N E_0(i) \\ E_0(i) = \{e_0(X_i, X_j) \mid j \in \Gamma_0(i)\} \\ \Gamma_0(i) = \left\{ j \mid j = \underset{X_h \in X}{\operatorname{argmin}} k(\{d(X_i, X_h), X_h \in X\}) \right\}. \end{cases} \quad (7)$$

Here, each player in the set X corresponds to a vertex in the network $G_0(X, E_0, d)$; E_0 is a link set and a link in the network represents certain relationship between a pair of players; the distances denote the weights over links; the function, $\operatorname{argmin} k(\cdot)$, is to find k nearest neighbors of a player which construct a neighbor set, $\Gamma_0(i)$; the subscript ‘0’ is the initial time step.

It is worth noting that the strength of links between a player X_i and his k nearest neighbors represented by $\rho_{t-1}(X_i, X_j)$, $j \in \Gamma_{t-1}(i)$ ($t \geq 1$) is time varying, whose initial value is calculated by

$$\rho_0(X_i, X_j) = \begin{cases} 1/|\Gamma_0(i)| = 1/k, & j \in \Gamma_0(i) \\ 0, & \text{otherwise,} \end{cases} \quad (8)$$

where the symbol $|\cdot|$ denotes the cardinality of a set.

After the initial connections are constructed among players (data points), on this weighted and directed knn network, a quantum game can be defined as follows.

Definition 2. A quantum game $\Omega = \{X, G_t, S, Z_t\}$ on a network G_t is a four-tuple: X is a set of players; G_t represents the connections among players; $S = \{s(i), i = 1, 2, \dots, N\}$ represents a set of players’ strategies including the full range of quantum strategies; $Z_t = \{z_t(i), i = 1, 2, \dots, N\}$ represents a set of players’ expected payoffs. Here, the variable t denotes the time step (the number of iterations). In each round, players choose their strategies simultaneously, and each player can only observe its neighbors’ payoffs but does not know the strategy profiles of all other players in X .

3.1. Cases of quantum strategies and payoff matrices

First, each player selects a strategy from his strategy set, and then plays a 2×2 entangled quantum game against one of his k neighbors, respectively. In the classical 2×2 game, such as the prisoners’ dilemma, usually there are only two pure strategies, cooperation and defection, but in the quantum game, one can design different unitary operators as strategies, i.e. the strategy set S may be identified with some subset of the group of 2×2 unitary matrices [6]. Here, for the purpose of clustering and simplifying computation, the strategy set of a player X_i is restricted in a set $S_1 = \{\hat{H}, \hat{D}\}$ or $S_2 = \{\hat{F}_{t-1}(i, j), \hat{D}\}$, and then two cases of strategy sets are described, respectively.

Case 1. In this case, a player and his opponent can apply strategies in $S_1 = \{\hat{H}, \hat{D}\}$. When a player X_i use the Hadamard matrix \hat{H} as a strategy, his opponent (neighbor) X_j has two optional strategies $\{\hat{H}, \hat{D}\}$, but which strategy is chosen is dependent on the strength of the link between them, as is a rule of the clustering algorithm. If the strength $\rho_{t-1}(X_j, X_i)$ equals zero, i.e. there is no link directed from the player X_j to the player X_i , then the player X_j will apply the strategy ‘defection’ (\hat{D}). Alternatively, if $\rho_{t-1}(X_j, X_i) > 0$, namely mutual connections between them, the player X_j implements the strategy \hat{H} . If the initial state of the

Table 2. PD-like payoff matrix.

	$C = 0$	$D = 1$
$C = 0$	$R = 0.6\omega_{t-1}(X_i, X_j)$	$S = 0.01\omega_{t-1}(X_i, X_j)$
$D = 1$	$T = \omega_{t-1}(X_i, X_j)$	$P = 0.2\omega_{t-1}(X_i, X_j)$

Table 3. SD-like payoff matrix.

	$C = 0$	$D = 1$
$C = 0$	$R = \omega_{t-1}(X_i, X_j) - \frac{c}{2}$	$S = \omega_{t-1}(X_i, X_j) - c$
$D = 1$	$T = \omega_{t-1}(X_i, X_j)$	$P = 0.01\omega_{t-1}(X_i, X_j)$

game is $|\psi_0\rangle = \hat{J}|00\rangle$, by applying the model of the quantum game the final state of the game is

$$|\psi_{f,j}\rangle = \begin{cases} \frac{1}{2}(|00\rangle - i|01\rangle - i|10\rangle + |11\rangle), & \hat{H} \otimes \hat{H} \\ \frac{1}{\sqrt{2}}(i|00\rangle - |01\rangle), & \hat{H} \otimes \hat{D}. \end{cases} \quad (9)$$

Case 2. The strategy set $S_2 = \{\hat{F}_{t-1}(i, j), \hat{D}\}$ is adopted in this case. The strategy $\hat{F}_{t-1}(i, j)$,

$$\hat{F}_{t-1}(i, j) = \begin{pmatrix} \sqrt{\rho_{t-1}(X_i, X_j)} & \sqrt{1 - \rho_{t-1}(X_i, X_j)} \\ \sqrt{1 - \rho_{t-1}(X_i, X_j)} & -\sqrt{\rho_{t-1}(X_i, X_j)} \end{pmatrix},$$

is a general form of Hadamard matrix \hat{H} whose elements are associated with the strength of links $\rho_{t-1}(X_i, X_j)$. When $\rho_{t-1}(X_i, X_j) = 0.5$, the strategy $\hat{F}_{t-1}(i, j)$ recovers the strategy \hat{H} . Similarly, the neighbor X_j , when $\rho_{t-1}(X_j, X_i) = 0$, applies the strategy ‘defection’ (\hat{D}), while using the strategy $\hat{F}_{t-1}(i, j)$ when $\rho_{t-1}(X_j, X_i) > 0$. If the initial state of the game is $|\psi_0\rangle = \hat{J}|00\rangle$, after their moves, the final state of the game is

$$|\psi_{f,j}\rangle = \begin{cases} \sqrt{\rho_1\rho_2}|00\rangle - i\sqrt{\rho_2(1 - \rho_1)}|01\rangle \\ -i\sqrt{\rho_1(1 - \rho_2)}|10\rangle + \sqrt{(1 - \rho_1)(1 - \rho_2)}|11\rangle, & \hat{F}_{t-1} \otimes \hat{F}_{t-1} \\ i\sqrt{1 - \rho_1}|00\rangle - \sqrt{\rho_1}|01\rangle, & \hat{F}_{t-1} \otimes \hat{D} \end{cases} \quad (10)$$

According to the payoff matrix, the player’s expected payoff can be computed by

$$\begin{aligned} z_{t-1}(i) &= \sum_{j \in \Gamma_{t-1}(i)} z_{t-1}(X_i, X_j) \\ &= \sum_{j \in \Gamma_{t-1}(i)} R|\langle\psi_{f,j}|00\rangle|^2 + S|\langle\psi_{f,j}|01\rangle|^2 + T|\langle\psi_{f,j}|10\rangle|^2 + P|\langle\psi_{f,j}|11\rangle|^2. \end{aligned} \quad (11)$$

In practice, the payoff matrix takes PD-like or Snowdrift (SD)-like form, described in tables 2 and 3. In the PD-like payoff matrix, the following inequalities hold: $T > R > P > S$ and $2R > T + S$ [28]. To avoid a case that a player’s expected payoff is zero, the variable S in table 2 takes a small value instead of zero in table 1. In addition, the Snowdrift game assumes that two drivers are blocked by a snowdrift, each of whom is in either side of the snowdrift. If they want to go back home, one of them or both must shovel a path through the snowdrift. So, there exists a cost c in the SD-like payoff matrix and the following inequality holds: $T > R > S > P$ [28], where $c = \beta \cdot \omega_{t-1}(X_i, X_j)$ and β is a proportional factor. Besides, the variable $\omega_{t-1}(X_i, X_j)$ in two payoff matrices is calculated by the formulation below:

$$\omega_{t-1}(X_i, X_j) = \rho_{t-1}(X_i, X_j) \times \text{Deg}_{t-1}(X_j)/d(X_i, X_j). \quad (12)$$

3.2. Design of LRR functions

When all players' payoffs have been computed, each player will observe his neighbors' payoffs and apply a link-removing-and-rewiring (LRR) function $L_i(\cdot)$ to change his links. A LRR function is defined as below.

Definition 3. The LRR function $L_i(\cdot)$ is a function of payoffs, whose output is a set with k elements, namely an updated neighbor set $\Gamma_t(i)$ of a player X_i . It is given as below:

$$\Gamma_t(i) = L_i(\hat{z}_{t-1}(i)) = \underset{j \in \Gamma_{t-1}(i) \cup \Upsilon_{t-1}(i)}{\operatorname{argmax}} k \left(\{z_{t-1}(j), j \in \Gamma_{t-1}(i) \cup \Upsilon_{t-1}(i)\} \right)$$

$$\hat{z}_{t-1}(i) = \{z_{t-1}(j), j \in \Gamma_{t-1}(i) \cup \Upsilon_{t-1}(i)\}, \quad \Upsilon_{t-1}(i) = \bigcup_{j \in \Gamma_{t-1}^+(i)} \Gamma_{t-1}(j) \quad (13)$$

$$\Gamma_{t-1}^+(i) = \{j | z_{t-1}(j) \geq \theta_{t-1}(i), j \in \Gamma_{t-1}(i)\}, \quad \Gamma_{t-1}^-(i) = \Gamma_{t-1}(i) \setminus \Gamma_{t-1}^+(i)$$

where $\theta_{t-1}(i)$ is a payoff threshold, $\Upsilon_{t-1}(i)$ is called an extended neighbor set and the function $\operatorname{argmax} k(\cdot)$ is to find k neighbors with the first k largest payoffs in the set $\Gamma_{t-1}(i) \cup \Upsilon_{t-1}(i)$.

Here, two LRR functions $L_i^1(\cdot)$ and $L_i^2(\cdot)$ are designed. The function $L_i^1(\cdot)$ always observes an extended neighbor set formed by half neighbors of a data point X_i , $\alpha = \lceil 0.5 \times |\Gamma_{t-1}(i)| \rceil$, where the symbol $\lceil \cdot \rceil$ is to take an integer part of a number satisfying that the integer part is no larger than the number. Next, the payoff threshold $\theta_{t-1}^1(i)$ is set by $\theta_{t-1}^1(i) = \operatorname{find}^\alpha(\{z_{t-1}(j), j \in \Gamma_{t-1}(i)\})$, where the function $\operatorname{find}^\alpha(\cdot)$ is to find the α th largest payoff in a set that contains all neighbors' payoffs of the data point. When the LRR function $L_i^1(\cdot)$ is applied, the links connecting the neighbors with small payoffs are removed and meanwhile new links are created between the data point and found players with higher payoffs. Hence, according to equation (13), the new neighbor set is $\Gamma_t(i) = L_i^1(\hat{z}_{t-1}(i))$.

Unlike the LRR function $L_i^1(\cdot)$, the LRR function $L_i^2(\cdot)$ adjusts the number of neighbors dynamically instead of the constant number of neighbors in $L_i^1(\cdot)$. Therefore, the payoff threshold $\theta_{t-1}^2(i)$ takes the average of neighbors' payoffs, $\theta_{t-1}^2(i) = \sum_{j \in \Gamma_{t-1}(i)} z_{t-1}(j) / |\Gamma_{t-1}(i)|$. Next, the set $\Gamma_{t-1}^+(i)$ is formed according to equation (13), $\Gamma_{t-1}^+(i) = \{j | z_{t-1}(j) \geq \theta_{t-1}^2(i), j \in \Gamma_{t-1}(i)\}$, and then the new neighbor set is achieved by means of the LRR function $L_i^2(\cdot)$, $\Gamma_t(i) = L_i^2(\hat{z}_{t-1}(i))$. In the case, when the payoffs of all neighbors are equal to the payoff threshold $\theta_{t-1}^2(i)$, the output of the LRR function is $\Gamma_t(i) = \Gamma_{t-1}(i)$. This may be viewed as self-protective behavior for avoiding a payoff loss due to not enough information acquired.

The LRR function $L_i(\cdot)$ expands the view of a player X_i , i.e. it makes him observe payoffs of players in the extended neighbor set, which provides a chance to find players with higher payoffs around him. If no players with higher payoffs are found in the extended neighbor set, namely $\min(\{z_{t-1}(j), j \in \Gamma_{t-1}(i)\}) \geq \max(\{z_{t-1}(h), h \in \Upsilon_{t-1}(i)\})$, then the output of the LRR function is $\Gamma_t(i) = \Gamma_{t-1}(i)$. Otherwise, players with small payoffs will be removed together with the corresponding links from the neighbor set and link set, and replaced by some found players with higher payoff. This process is repeated till the payoffs of unlinked players in the extended neighbor set are no larger than those of linked neighbors. Since the links among players, namely the link set E_0 in the network $G_0(X, E_0, d)$, are changed by the LRR function, the network $G_t(X, E_t, d)$ has begun to evolve over time, when $t \geq 1$:

$$G_t(X, E_t, d) = \begin{cases} X(t) = \{X_i(t), i = 1, 2, \dots, N\} \\ \Gamma_t(i) = L_i(\hat{z}_{t-1}(i)) \\ E_t = \bigcup_{i=1}^N E_t(i) \\ E_t(i) = \{e_t(X_i, X_j) \mid j \in \Gamma_t(i)\}. \end{cases} \quad (14)$$

3.3. Strength of links updating

After the LRR function is applied, the strength of links of players needs to be formed and adjusted. The new strength of links of a player $X_i \in X$ is formed by means of the below formulation:

$$\rho_t(X_i, X_j) = \begin{cases} \frac{\sum_{h \in \Gamma_{t-1}(i) \setminus \{\Gamma_{t-1}(i) \cap \Gamma_t(i)\}} \rho_{t-1}(X_i, X_h)}{|\Gamma_t(i) \setminus \{\Gamma_{t-1}(i) \cap \Gamma_t(i)\}|} & j \in \Gamma_t(i) \setminus \{\Gamma_{t-1}(i) \cap \Gamma_t(i)\} \\ \rho_{t-1}(X_i, X_j) & \text{otherwise.} \end{cases} \quad (15)$$

Then, the player adjusts the strength of links as follows. First, he finds a neighbor X_m with the maximal payoff in his neighbor set:

$$m = \operatorname{argmax}_{j \in \Gamma_t(i)} (z_{t-1}(j), j \in \Gamma_t(i)). \quad (16)$$

Next, the strength of link $\rho_t(X_i, X_j)$, $j \in \Gamma_t(i)$ is taken as its square root and the player X_m 's strength of the link becomes negative:

$$\begin{cases} \{\sqrt{\rho_t(X_i, X_j)}, j \in \Gamma_t(i)\} \\ \sqrt{\rho_t(X_i, X_m)} = -\sqrt{\rho_t(X_i, X_m)}, & m \in \Gamma_t(i) \end{cases} \quad (17)$$

Further, let $\operatorname{Ave}_t(i) = (\sum_{j \in \Gamma_t(i)} \sqrt{\rho_t(X_i, X_m)}) / |\Gamma_t(i)|$; thus, the updated strength of the link is

$$\rho_t(X_i, X_j) = (2 \times \operatorname{Ave}_t(i) - \sqrt{\rho_t(X_i, X_j)})^2, \quad j \in \Gamma_t(i). \quad (18)$$

The above-mentioned method is a variant of the Grover iteration G in the quantum search algorithm [3], a well-known algorithm in quantum computation, which is a way to adjust the probability amplitude of each term in a superposition state. By adjustment, the probability amplitude of the wanted is increased, while the others are reduced. This whole process may be regarded as the *inversion about average* operation [3]. For our case, each strength of the link is taken as its square root first, and then the average $\operatorname{Ave}_t(i)$ of square roots is computed. Finally, all values are inverted about the average. There are three main reasons why we selected the modified Grover iteration to update the strength of links: (a) the sum of updated strength of links retains one, $\sum_{j \in \Gamma_t(i)} \rho_t(X_i, X_j) = 1$, (b) certain strength of links between a player and his neighbors is much larger than the others, $\rho_t(X_i, X_j) \gg \rho_t(X_i, X_h)$, $h \in \Gamma_t(i) \setminus j$, after the strength of links is updated and (c) it helps players' payoffs to follow a power law distribution, in which only a few players' payoffs are far larger than others' in the end of iterations.

Besides, the process that all players adjust their strength is order irrelevant, because the strength of links of all players is updated synchronously, and the network is a directed network, so the strength cannot be overridden by other players. When the strength of links of each player has been updated, an iteration is completed. In conclusion, when $t \geq 1$, the structure of network representing connections among players begins to evolve over time.

4. Discussions

In this section, first the relationship between the number of nearest neighbors and the number of clusters is discussed, and then how the cost in the SD-like payoff matrix influences the results is analyzed, which provides a way to choose the proportional factor. Finally, the total payoffs based on two different payoff matrices are compared and the relationship between the total payoffs and the rates of convergence of algorithms is explained.

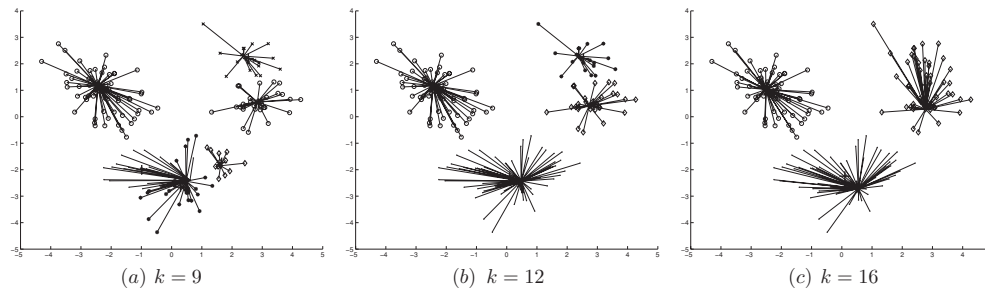


Figure 2. The number of nearest neighbors versus the number of clusters. (a) Six clusters are obtained, when the number of nearest neighbors is $k = 9$, (b) four clusters, when $k = 12$ and (c) three clusters, when $k = 16$.

4.1. Number of nearest neighbors versus the number of clusters

The number k of nearest neighbors represents the number of neighbors to which a data point (player) $X_i \in X$ connects. For a dataset, the number k of nearest neighbors determines the number of clusters in part. Generally speaking, the number of clusters decreases inversely with the number k of nearest neighbors. For example, when the number k of nearest neighbors is small, it is indicated that the player X_i connects to only a few neighbors. At this time only those not-too-distance neighbors can be observed by the LRR function, which means that the elements in the union of the extended neighbor set $\Upsilon_{t-1}(i)$ and the neighbor set $\Gamma_{t-1}(i)$ are few. Therefore, when the evolution of the network formed by players is ended, many small clusters are established among data points. On the other hand, a big number k of nearest neighbors provides more neighbors for each player, as it specifies that the cardinality of the union is larger than that when a small k is taken. This means that more neighbors can be observed and explored by the LRR function, so that big clusters containing more data points are formed.

For a dataset, the clustering results at the different number k of nearest neighbors have been illustrated in figure 2, in which each data point only connects to one of its neighbors who has the largest strength of link, and clusters are represented by different signs. As is shown in figure 2, it can be found that only a few data points receive considerable links, whereas most of the data points have only one link. This implies that when the structure of network tends to stability, the network, if only the links with the largest strength are remained, is characterized by the scale-free network [29], i.e. winner takes all. Besides, in figure 2(a), six clusters are obtained by the clustering algorithm, when $k = 9$. As the number k of nearest neighbors rises, four clusters are obtained when $k = 12$ and three clusters when $k = 16$. So, if the exact number of clusters is not known in advance, different numbers of clusters may be achieved by adjusting the number of nearest neighbors in practice.

4.2. Effect of the cost c in the SD-like payoff matrix

In the Snowdrift game, if the cost is too high, the SD-like payoff matrix recovers the PD-like payoff matrix [28]. Therefore, the proportional factor β is restricted in an interval $(0, 0.5]$. However, different costs will bring about the changes of the payoff matrix, which means that different clustering results will be produced even in the same algorithm. Figure 3 illustrates how the clustering results change at the different number k of nearest neighbors when the

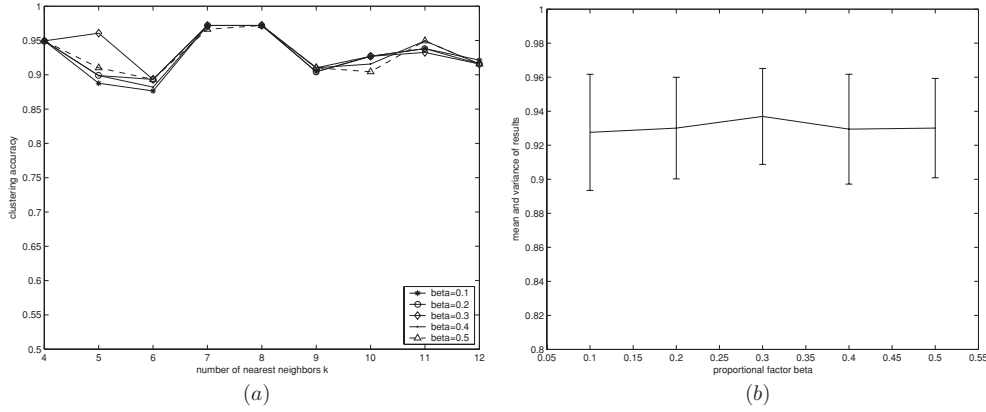


Figure 3. The effect of the cost for the clustering results. (a) The results of the algorithm using the SD-like payoff matrix at different number k of nearest neighbors. (b) The mean and variance corresponding to each curve in (a).

proportional factor β takes different values, in which the clustering results are represented by clustering accuracies. The definition of clustering accuracy is given below.

Definition 4. $Cluster_i$ is the label which is assigned to a data point X_i in a dataset by the algorithm, and $label_i$ is the actual label of the data point X_i in the dataset. So the clustering accuracy is [30]:

$$accuracy = \frac{\sum_{i=1}^N \lambda(\text{map}(\text{cluster}_i), \text{label}_i)}{N} \tag{19}$$

$$\lambda(\text{map}(\text{cluster}_i), \text{label}_i) = \begin{cases} 1 & \text{if } \text{map}(\text{cluster}_i) = \text{label}_i \\ 0 & \text{otherwise} \end{cases}$$

where the mapping function $\text{map}(\cdot)$ maps the label got by the algorithm to the actual label.

Clustering accuracy is an important evaluation criterion for clustering algorithms, which reflects the level of matches between the actual labels in a dataset and the labels assigned by a clustering algorithm, so that the goal of a clustering algorithm is to obtain higher clustering accuracies.

As is shown in figure 3, it can be seen that similar results are obtained by the algorithm at different costs, and the best results are produced when $k = 7$ and $k = 8$, but from figure 3(b), the clustering result with the largest mean and the least variance is yielded when $\beta = 0.3$. Also, as mentioned above, the high cost leads to the recovery of the SD-like payoff matrix, so the proportional factor $\beta = 0.2$ or $\beta = 0.3$ is recommended.

4.3. Total payoffs and the rate of convergence

In this subsection, first the total payoffs of algorithms using the PD- or SD-like payoff matrix are compared respectively, and then the differences between total payoffs are explained. Later, the rates of convergence of algorithms are discussed when two LRR functions are applied respectively, and further the impact for the rates of convergence is analyzed in two payoff matrices.

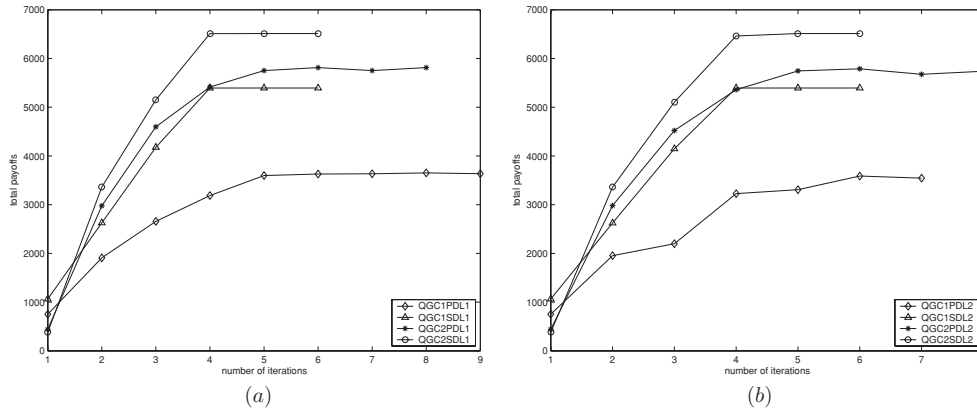


Figure 4. The total payoffs versus the rates of convergence. (a) Total payoffs of algorithms in the case of LRR function $L_i^1(\cdot)$; (b) total payoffs of algorithms in the case of LRR function $L_i^2(\cdot)$.

Remark 1. The algorithms are named as follows. For example, the name of an algorithm, QGC1PDL1, denotes that the case 1, PD-like payoff matrix and the LRR function $L_i^1(\cdot)$ are employed in this algorithm.

If all other conditions are fixed, an algorithm will form two versions due to using PD- or SD-like payoff matrix, and naturally this will bring different results. As compared with the PD-like payoff matrix, the payoff P and S in the SD-like payoff matrix have a reverse order in the payoff inequality. In all algorithms, the relationship between the total payoffs and the number of iterations is drawn in figure 4. From figure 4, it can be found that the total payoffs in the algorithms with the SD-like payoff matrix are larger than that of the algorithms with the PD-like payoff matrix no matter which LRR function is selected.

According to two payoff matrices, using equation (11), each player’s expected payoff can be calculated in two cases of strategies, respectively, as below:

case 1:

$$PD : z_t(X_i, X_j) = \begin{cases} \frac{1}{4}(0.6\omega + 0.01\omega + \omega + 0.2\omega) = 0.4525\omega \\ \frac{1}{2}(0.6\omega + 0.01\omega) = 0.305\omega \end{cases} \tag{20}$$

$$SD : z_t(X_i, X_j) = \begin{cases} \frac{1}{4}\left(\omega - \frac{c}{2} + \omega - c + \omega + 0.01\omega\right) = \frac{1}{4}\left(3.01 - \frac{3\alpha}{2}\right)\omega \\ \frac{1}{2}\left(\omega - \frac{c}{2} + \omega - c\right) = \frac{1}{2}\left(2 - \frac{3\alpha}{2}\right)\omega; \end{cases} \tag{21}$$

case 2:

$$PD : z_t(X_i, X_j) = \begin{cases} \rho_1\rho_2 0.6\omega + \rho_2(1 - \rho_1)0.01\omega \\ + \rho_1(1 - \rho_2)\omega + (1 - \rho_1)(1 - \rho_2)0.2\omega \\ (1 - \rho_1)0.6\omega + \rho_1 0.01\omega \end{cases} \tag{22}$$

$$SD : z_t(X_i, X_j) = \begin{cases} \rho_1 \rho_2 \left(\omega - \frac{c}{2} \right) + \rho_2 (1 - \rho_1) (\omega - c) \\ \quad + \rho_1 (1 - \rho_2) \omega + (1 - \rho_1) (1 - \rho_2) 0.01 \omega \\ (1 - \rho_1) \left(\omega - \frac{c}{2} \right) + \rho_1 (\omega - c). \end{cases} \quad (23)$$

Comparing the expected payoffs in two cases, it can be observed that when the SD-like payoff matrix is used, the expected payoff is larger than that of using PD-like payoff matrix regardless of cases of strategies. Therefore, this explains why differences between total payoffs are produced.

Besides, figure 4 not only describes the changes of total payoffs of algorithms but also reflects the rates of convergence of algorithms. When the total payoffs remain constant or fluctuate slightly, this means that the algorithms have converged. At this time, players do not frequently apply the LRR function to change his neighbors but reach a stable state. As mentioned in section 3.2, the LRR function $L_i^2(\cdot)$ only can observe an extended neighbor set formed by those larger-than-average neighbors in contrast to an extended neighbor set built by half neighbors in the LRR function $L_i^1(\cdot)$. Generally speaking, for the same k , the median of payoffs is smaller than or equal to the mean, i.e. $\theta_{t-1}^1 \leq \theta_{t-1}^2$, which means that the exploring area of the LRR function $L_i^1(\cdot)$ is larger than that of the LRR function $L_i^2(\cdot)$. So, as a whole, the algorithms with the LRR function $L_i^2(\cdot)$ are slightly faster than that with the LRR function $L_i^1(\cdot)$, i.e. the number of iterations that the former type of algorithms needs is a little less.

Furthermore, in the algorithms, a phenomenon that the strategies \hat{H} and \hat{F}_{t-1} are more likely used by players in a high-density area while the strategy \hat{D} is used by those in a low-density area is always observed. This is because usually they are mutual neighbors in the high-density area on the weighted and directed knn network, but in the low-density area this case is reverse. As a result, the differences of payoffs between the high-density and low-density areas are enlarged rapidly for the expected payoff in the strategy profile (\hat{H}, \hat{H}) or $(\hat{F}_{t-1}, \hat{F}_{t-1})$ is higher than that in other strategy profile, and this also causes the distribution of players' payoffs follow a power-law distribution, which is why algorithms converge fast.

5. Simulations

To evaluate these clustering algorithms, six datasets are selected from the UCI repository [31], which are Soybean, Iris, Wine, Sonar, Ionosphere and Breast cancer Wisconsin datasets, and the simulations are completed on them. In this section, first these datasets are briefly introduced, and then the simulation results are demonstrated.

The original data points in the above datasets are all scattered in high-dimensional spaces spanned by their features which are the individual measurable heuristic properties of the phenomena being observed, where the description of all datasets is summarized in table 4. As for Breast dataset, some lost features are replaced by random numbers, and the Wine dataset is standardized. Finally, the algorithms are coded in Matlab 6.5.

Throughout all simulations, data points in a dataset are viewed as players in quantum games whose initial positions are taken from the dataset. Next, the initial network representing relations among data points are created according to definition 1, after a distance function is selected, which only needs to satisfy that the more similar the data points, the smaller the output of the function is. In the simulations, the distance function is employed as follows:

$$d(X_i, X_j) = \exp(\|X_i - X_j\|/2\sigma^2), \quad i, j = 1, 2, \dots, N, \quad (24)$$

where the symbol $\|\cdot\|$ represents the L_2 -norm. The advantage of this function is that it not only satisfies our requirements but also overcomes the drawbacks of Euclidean distance. For

Table 4. Description of datasets.

Dataset	Instances	Features	Classes
Soybean	47	21	4
Iris	150	4	3
Wine	178	13	3
Sonar	208	60	2
Ionosphere	351	32	2
Breast	699	9	2

instance, when two points are very close, the output of Euclidean distance function approaches zero, which may make the computation of payoff fail due to the payoff approaching infinite. Nevertheless, when equation (24) is selected as the distance function, it is more convenient to compute the players' payoffs, since its minimum is 1 and the reciprocals of its output are between 0 and 1, $1/d(X_i, X_j) \in [0, 1]$.

In addition, the distance between a player X_i and itself, $d(X_i, X_i)$, is 1 according to the defined distance function, which means that initially he is one of his k nearest neighbors. So there is an edge between the player X_i and himself, namely a self-loop. Additionally, the parameter σ in equation (24) takes 1. As is analyzed in section 4.2, the cost c in SD-like payoff matrix is set by $c = 0.2\omega_i(X_i, X_j)$ in the related clustering algorithms.

The clustering algorithms are applied on the six datasets, respectively. Because two cases of strategies are designed and the different payoff matrices and LRR functions are employed, the algorithms are run on every dataset at the different number k of nearest neighbors. As is analyzed in section 4.1, for a dataset the number k of clusters decreases inversely with the number of nearest neighbors. When a small k is selected, it is possible that the number of clusters is larger than the preset number of the dataset, after the algorithm is ended. So a merging subroutine is called to merge unwanted clusters, which works in this way. At first, the cluster with the fewest data points is identified, and then it is merged to the cluster whose distance between their centroids is smallest. This subroutine is repeated till the number of clusters is equal to the preset number.

The clustering results obtained by these algorithms are compared in figure 5, in which each point represents a clustering accuracy. As is shown in figure 5, the similar results are obtained by these algorithms at different number of nearest neighbors, but almost all the best results are obtained by the algorithms using the LRR function $L_i^1(\cdot)$.

Further, we show a simple comparison with three other algorithms: Kmeans [32, 33], PCA-Kmeans [33], LDA-Km [33]. The Kmeans algorithm is a popular clustering algorithm because it is easy to implement. It begins with k randomly chosen cluster centers, and then assigns each data point in a dataset to the closest cluster center. Next, the cluster centers are recomputed according to the current cluster memberships. This process will be repeated till a convergence criterion is met. However, its major problem is sensitive to the selection of the initial partition [19]. The PCA-Kmeans algorithm consists of two steps: (1) reducing the data dimension by principal component analysis (PCA), (2) clustering data points by the Kmeans algorithm. Ding *et al* combine linear discriminant analysis (LDA) with the Kmeans algorithm and construct a new clustering algorithm called 'LDA-Km'. In the LDA-Km algorithm, Kmeans is used to generate class labels, while LDA is used to do subspace selection. Finally, in the subspace selection process, data points are clustered.

Our algorithms are established on the model of quantum games, so data points in datasets are considered as players. This idea is totally different from traditional clustering algorithms,

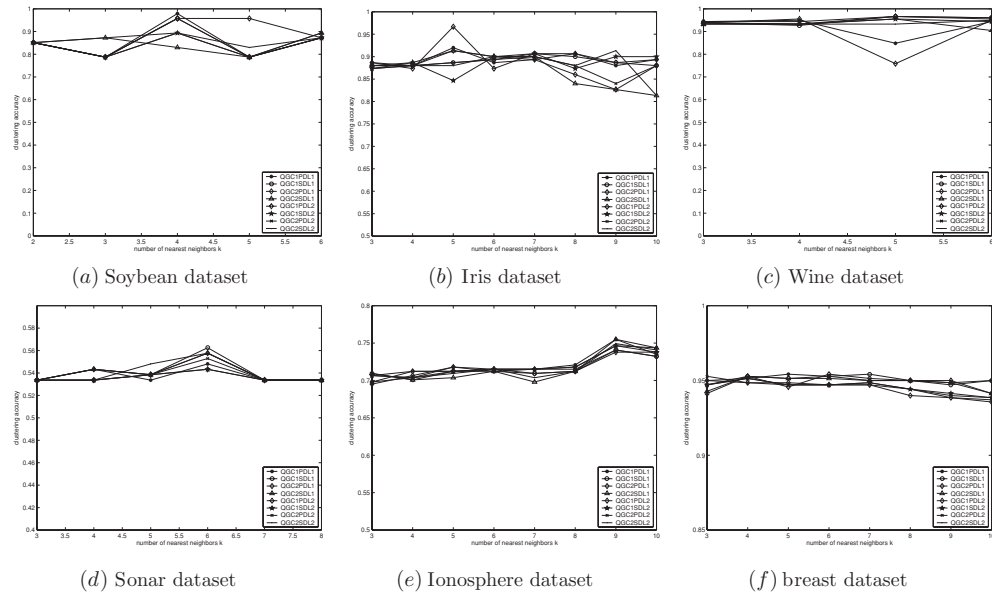


Figure 5. Comparison of clustering accuracies at different k in all proposed algorithms.

Table 5. Comparison of clustering accuracies of algorithms.

Algorithm	Soybean	Iris	Wine	Sonar	Ionosphere	Breast
QGC1PDL1	97.9%	92.0%	94.9%	54.8%	75.5%	95.4%
QGC1SDL1	95.6%	90.7%	96.6%	56.3%	74.1%	95.4%
QGC2PDL1	95.6%	91.3%	96.6%	55.8%	73.8%	95.4%
QGC2SDL1	89.4%	91.3%	96.6%	55.8%	75.5%	95.3%
QGC1PDL2	95.8%	96.7%	95.5%	54.3%	74.1%	95.0%
QGC1SDL2	89.4%	90.7%	95.5%	54.3%	74.6%	95.1%
QGC2PDL2	89.4%	90.0%	95.5%	55.3%	74.6%	95.3%
QGC2SDL2	89.4%	91.3%	94.9%	55.8%	74.9%	95.1%
Kmeans [33]	68.1%	89.3%	70.2%	47.2%	71.0%	–
PCA-Kmeans [33]	72.3%	88.7%	70.2%	45.3%	71.0%	–
LDA-Km [33]	76.6%	98.0%	82.6%	51.0%	71.2%	–

such as Kmeans and its variants, because in traditional clustering algorithms data points for clustering are fixed, and various functions or methods are designed to find cluster centers or separating hyperplanes, whereas in the quantum-game-based clustering algorithms data points (players) themselves choose their clusters, which leads clusters to be formed automatically during quantum games. In conclusion, traditional clustering algorithms do it from outside, while ours are from inside. Furthermore, our algorithms do not need to choose cluster centers at the beginning, so there does not exist the problem that is ‘sensitive to the selection of the initial partition’. Besides, distances between data points are commonly used as the measurement of their similarities in the Kmeans algorithm and its variants. However, when similarities are measured in our algorithms, not only distances between data points but also their degrees and the strength of links are integrated, which provides more information for the measurement

of similarities. Later, according to payoffs in quantum games, players apply a LRR function to change the structure of the network, which makes the clusters emerge. As a result, better clustering accuracies are obtained by our algorithms.

Table 5 displays the clustering accuracies of our algorithms and the other three algorithms using the datasets in table 4. It can be observed that on almost all datasets the quantum-game-based clustering algorithms have the best clustering accuracies. Only on the Iris dataset, the LDA-Km algorithm is better than ours, but our result is close to it as well. The Iris dataset contains three clusters, one of which is far from the other two, so data points in it can be clustered easily and correctly. The other clusters in the Iris dataset, however, are mixed partly in their boundaries, which brings a difficulty for clustering. These mixed boundary points may be assigned to different clusters by algorithms, which is why the clustering accuracies of algorithms are various. It is more difficult to cluster data points in the Sonar and Ionosphere dataset, because in these two datasets plenty of data points belonging to different clusters are mixed together. Therefore, the clustering accuracies of algorithms in them are not high, and it is rather hard to improve the clustering accuracies even by several percents. From the fifth and sixth columns in table 5, it can be seen that the quantum-game-based clustering algorithms are better than other algorithms, which indicates the effectiveness of our algorithms.

6. Conclusions

The enormous successes gained by quantum algorithms makes us realize that it is possible that quantum algorithms can obtain solutions faster and better than classical algorithms for some problems. Therefore, we combine quantum game with the problem of data clustering, and establish clustering algorithms based on quantum games. In the algorithms, data points for clustering are regarded as players who can make decisions in quantum games. On a weighted and directed knn network that represents the relations among players, each player uses quantum strategies against every one of his neighbors in a 2×2 entangled quantum game, respectively. We design two cases of strategies: (i) one plays the strategy \hat{H} , the other plays the strategy \hat{H} or \hat{D} , (ii) one plays the strategy \hat{F}_{t-1} , the other plays the strategy \hat{F}_{t-1} or \hat{D} according to the strength of links, in each of which players' expected payoffs are calculated based on the PD- and SD-like payoff matrices, respectively. According to the neighbors' payoffs in one's neighbor set, each player applies a LRR function ($L_i^1(\cdot)$ or $L_i^2(\cdot)$) to change his neighbors, i.e. the links connecting to neighbors with small payoffs are removed and then new links are created to those with higher payoffs. Later, the Grover iteration G is employed to update the strength of links between him and his neighbors. In the process of playing quantum game, the structure of the network formed by players tends to stability gradually. In other words, each player always connects to one of his neighbors with the largest strength or jumps among some neighbors with the largest strength in a constant period. At this time, if only the links with the largest strength are left but all other links are removed among players, the network naturally divides into several separate parts, each of which corresponds to a cluster.

Additionally, in simulations, it can be found that the total expected payoffs of algorithms using the SD-like payoff matrix are higher than that of algorithms using the PD-like payoff matrix. Later, the reason is explained. Further, we observe that the rates of convergence of the algorithms employing the LRR function $L_i^2(\cdot)$ are faster slightly than that of the algorithms employing the LRR function $L_i^1(\cdot)$, because more areas are explored by the LRR function $L_i^1(\cdot)$, but this brings better clustering results. In the case when the exact number of clusters is unknown in advance, one can adjust the number k of nearest neighbors to control the

number of clusters, where the number of clusters decreases inversely with the number k of nearest neighbors. Finally, the clustering algorithms are evaluated on six real datasets, and simulation results have demonstrated that data points in a dataset are clustered reasonably and efficiently.

Acknowledgments

The authors would like to thank the anonymous referees for their helpful comments and suggestions to improve the presentation of this paper. This work was supported in part by the National Natural Science Foundation of China (no 60405012, no 60675055).

References

- [1] Vedral V and Plenio M 1998 *Prog. Quantum Electron.* **22** 1–39
- [2] Shor P W 1994 *1994 Proc. of the 35th Ann. Symp. on Foundations of Computer Science* pp 124–34
- [3] Grover L K 1997 *Phys. Rev. Lett.* **79** 325
- [4] Brassard G, Høyer P and Tapp A 1998 *Automata, Languages and Programming (Lecture Notes in Computer Science vol 1443)* (Berlin: Springer) pp 820–31
- [5] Meyer D A 1999 *Phys. Rev. Lett.* **82** 1052
- [6] Eisert J, Wilkens M and Lewenstein M 1999 *Phys. Rev. Lett.* **83** 3077
- [7] Flitney A P and Abbott D 2003 *Proc. R. Soc. B* **459** 2463
- [8] Marinatto L and Weber T 2000 *Phys. Lett. A* **272** 291–303
- [9] Lee C F and Johnson N F 2003 *Phys. Rev. A* **67** 022311
- [10] Du J, Li H, Xu X, Shi M, Wu J, Zhou X and Han R 2002 *Phys. Rev. Lett.* **88** 137902
- [11] Prevedel R, Stefanov A, Walther P and Zeilinger A 2007 *N. J. Phys.* **5** 205–15
- [12] Schmid C, Flitney A P, Wieczorek W, Kiesel N, Weinfurter H and Hollenberg L C L 2009 arXiv:0901.0063v1
- [13] Guo H, Zhang J and Koehler G J 2008 *Decis. Support Syst.* **46** 318–32
- [14] Horn D and Gottlieb A 2001 *Phys. Rev. Lett.* **88** 018702
- [15] Sasaki M and Carlini A 2002 *Phys. Rev. A* **66** 022303
- [16] Trugenberger C A 2002 *Quantum Inf. Process.* **1** 471–93
- [17] Schützhold R 2003 *Phys. Rev. A* **67** 062311
- [18] Aïmeur E, Brassard G and Gambs S 2007 *Proc. of the 24th Int. Conf. on Machine Learning (Corvallis, OR)*
- [19] Jain A K, Murty M N and Flynn P J 1999 *ACM Comput. Surv.* **31** 264–323
- [20] Ekert A, Hayden P M and Inamori H 2001 *Coherent Atomic Matter Waves vol 72* (Berlin: Springer) p 661
- [21] Nielsen M A and Chuang I L 2000 *Quantum Computation and Quantum Information* (Cambridge: Cambridge University Press)
- [22] Nash J 1950 *Proc Natl Acad. Sci.* **36** 48–9
- [23] Nash J 1951 *Ann. Math.* **54** 286–95
- [24] Fudenberg D and Tirole J 1983 *Game Theory* (Cambridge, MA: MIT Press)
- [25] Benjamin S C and Hayden P M 2001 *Phys. Rev. A* **64** 030301
- [26] Du J, Li H, Xu X, Shi M, Zhou X and Han R 2001 arXiv:quant-ph/0111138
- [27] Du J, Li H, Xu X, Zhou X and Han R 2003 *J. Phys. A: Math. Gen.* **36** 6551–62
- [28] Hauert C and Doebeli M 2004 *Nature* **428** 643–6
- [29] Barabási A L and Bonabeau E 2003 *Sci. Am.* **288** 60–9
- [30] Erkan G 2006 *Proc. of the Main Conf. on Human Language Technology, Conference of the North American Chapter of the Association of Computational Linguistics* (New York: Association for Computational Linguistics)
- [31] Asuncion A and Newman D J 2007 *UCI Machine Learning Repository* (Irvine, CA: University of California, School of Information and Computer Science) <http://www.ics.uci.edu/~mlearn/MLRepository.html>
- [32] MacQueen J 1967 *Proc. of 5th Berkeley Symp. on Mathematical Statistics and Probability vol 1* (Berkeley, CA: University of California Press) pp 281–97
- [33] Ding C and Li T 2007 *Proc. of the 24th Int. Conf. on Machine Learning (Corvallis, OR)* pp 521–8